

Montclair State University

Montclair State University Digital Commons

Theses, Dissertations and Culminating Projects

5-2020

Stochastic Modeling of Zoonotic Disease

Sausan Odatalla

Montclair State University

Follow this and additional works at: <https://digitalcommons.montclair.edu/etd>

 Part of the [Applied Mathematics Commons](#)

Recommended Citation

Odatalla, Sausan, "Stochastic Modeling of Zoonotic Disease" (2020). *Theses, Dissertations and Culminating Projects*. 474.

<https://digitalcommons.montclair.edu/etd/474>

This Thesis is brought to you for free and open access by Montclair State University Digital Commons. It has been accepted for inclusion in Theses, Dissertations and Culminating Projects by an authorized administrator of Montclair State University Digital Commons. For more information, please contact digitalcommons@montclair.edu.

Abstract

We provide an overview of the mathematical modeling of deterministic and stochastic infectious disease models. These models enable one to understand the outbreak, spread, and extinction of disease. We then focus on stochastic models with a disease reservoir to understand outbreak vulnerability for zoonotic diseases such as Ebola Virus Disease (EVD). Numerical results from a more complicated EVD model are compared with the theoretical results of a simplified stochastic SIS_κ model. We also demonstrate the effect that vaccine has on outbreak vulnerability in a population that is connected to a disease reservoir.

MONTCLAIR STATE UNIVERSITY

Stochastic Modeling of Zoonotic Disease

by

Sausan Odatalla

A Master's Thesis Submitted to the Faculty of

Montclair State University

In Partial Fulfillment of the Requirements

For the Degree of

Master of Science

May 2020

College of Science and Mathematics

Department of Applied
Mathematics and Statistics

Thesis Committee:

[Redacted]

Dr. Eric Forgoston

Thesis Sponsor

[Redacted]

Dr. Lora Billings

Committee Member

[Redacted]

Dr. David Trubatch

Committee Member

STOCHASTIC MODELING OF ZOO NOTIC DISEASE

A THESIS

Submitted in partial fulfillment of the requirements

For the degree of Master of Science

by

SAUSAN ODATALLA

Montclair State University

Montclair, NJ

2020

Contents

1	Introduction	6
1.1	History of Mathematical Epidemiology	6
2	Theory and Background	8
2.1	Compartmental models	8
2.1.1	Susceptible-Infectious-Recovered (SIR) Model:	9
2.1.2	Susceptible-Infectious-Susceptible (SIS) Model	10
2.1.3	Susceptible-Exposed-Infectious-Recovered-Susceptible (SEIRS) Model	11
2.2	Deterministic Models	12
2.2.1	Theoretical Analysis - An Example	12
3	Stochastic Models	13
3.1	Master Equation and Internal Noise	13
3.2	Gillespie Algorithm	15
3.3	Complex Example: The Ebola Model	16
4	Stochastic Zoonotic SIS Models	20
4.1	Susceptible-Infectious-Susceptible- κ (SISκ) Model	20
4.2	Susceptible-Infectious-Susceptible- κ (SISκ) Model with Vaccine	24
5	Summary	29
6	Bibliography	30

List of Figures

1	Schematic of the <i>SIR</i> compartmental model.	9
2	Schematic of the <i>SIS</i> compartmental model.	10
3	Schematic of the <i>SEIRS</i> compartmental model.	11
4	Infectious individuals in time for the SIS model. The red curve is a single stochastic trajectory showing fluctuations about the deterministically stable endemic state (black line) before the eventual extinction. The parameter values are: $\mu = 0.9$, $\gamma = 0.1$, $\beta = 1.4$, and $N = 100$	16
5	Schematic of the Ebola Virus Disease (EVD) compartmental model.	17
6	Outbreak vulnerability in the EVD model showing different outbreak scenarios. The figure is taken from Ref.	18
7	Schematic of the <i>SISκ</i> compartmental model.	20
8	Probability density functions of the stochastic <i>SISκ</i> model for a range of N and κ values. The figure is taken from Ref. Parameter values are $\beta = 0.1$, $\gamma = 0.33$, and $\mu = 5.0 \times 10^{-5}$	22
9	Stochastic realizations of the <i>SISκ</i> model for a range of N and κ values. Parameter values are $\beta = 0.1$, $\gamma = 0.33$, and $\mu = 5.0 \times 10^{-5}$	23
10	Schematic of the <i>SIS$\kappa - V$</i> compartmental model.	24
11	Stochastic <i>SIS$\kappa - V$</i> realizations with 10% to 90% vaccination rates for varying N and κ values. Each sub-figure shows nine stochastic realizations with each sub-figure showing results for different values of c ranging from $c = 10\%$ to $c = 90\%$ increasing in uniform increments of size 10% from top to bottom, and left to right.	26
12	Stochastic <i>SIS$\kappa - V$</i> realizations with 1% to 9% vaccination rates for varying N and κ values. Each sub-figure shows nine stochastic realizations with each sub-figure showing results for different values of c ranging from $c = 1\%$ to $c = 9\%$ increasing in uniform increments of size 1% from top to bottom, and left to right.	27
13	Stochastic <i>SIS$\kappa - V$</i> realizations with 91% to 99% vaccination rates for varying N and κ values. Each sub-figure shows nine stochastic realizations with each sub-figure showing results for different values of c ranging from $c = 91\%$ to $c = 99\%$ increasing in uniform increments of size 1% from top to bottom, and left to right.	28

”The single biggest threat to man’s continued dominance on the planet is the virus.”

Joshua Lederberg, Nobel laureate in Physiology and Medicine

1 Introduction

Epidemiology comes from the Greek words *epi*, *demo*, and *logy* which mean “upon”, “the common people”, and “study” respectively. When combined, epidemiology becomes “the study of that which falls upon the common people.” The modern day definition is the study of the distribution and determinants of disease frequency in human populations and the application of this study to control health problems [1]. Epidemiology is a vital tool in the public health industry. It is a cross-disciplinary field combining knowledge from biologists, mathematicians, statisticians, engineers and computer scientists, to name just a few. According to the U.S. Centers for Disease Control and Prevention (CDC), epidemiology serves five core functions: public health surveillance, field investigation, analytic studies, evaluation, and linkages. Epidemiologists perform public health surveillance by collecting and monitoring incoming data. In particular, they analyze and interpret the data to see if anything is out of the ordinary. Epidemiologists also conduct relevant tests if any data analysis suggests more investigation is required. Sometimes this involves field investigations to look for additional cases. Other analytical work involves the development of epidemic models which provide predictions and possible trajectory paths based on preliminary results from field investigations. Finally, epidemiologists evaluate their results and link their discoveries and research with other organizations and public health workers to best assess the spread of a disease and different methods of containment [2].

Epidemiologists around the world use different data analysis methods in hopes of understanding the cause of an outbreak. They study the origin of the outbreak, spread patterns, and the optimal way to slow and eventually eradicate the disease. Epidemiologists also examine the possible source of a disease such as water, soil, plants, animals, or human made toxins. They investigate all classes of diseases, whether chronic, contagious, infectious or non-infectious. Epidemiologists use models to better understand key characteristics of disease spread and the most dynamically important trajectories of the spread. While human behavior is erratic and unpredictable to some extent, there has been much success in using different modeling approaches to better understand the outbreak and spread of infectious disease. In light of the COVID-19 world-wide epidemic, this thesis will shed some light onto the history, development, and modern day modeling techniques epidemiologists and other scientists use to process information and understand the outbreak and spread of diseases.

1.1 History of Mathematical Epidemiology

Infectious diseases have affected human populations for centuries. To limit the extent of disease spread, the number of individuals who become infected, and the number of individuals who die, scientists have developed different models to help explain the outbreak and spread of infectious disease, and to understand the effect of control measures on disease spread. One of the first individuals who tried to explain and predict the spread of disease was John Graunt, who performed his studies in London at the time of King Charles II. Graunt published his “Natural and Political Observations Made upon the Bills of Mortality” [3] after analyzing weekly death reports when the city was infected with the bubonic plague. His work did not model nor explain the outbreak and

spread of disease, but it was one of the first completely statistical pieces that kept track of the infected and non-infected populations of London at the time.

In 1766, Daniel Bernoulli used statistical data in “An attempt at a new analysis of the mortality caused by smallpox and of the advantages of inoculation to prevent it” [4] where he modeled the growth of the population with vaccines to persuade people of the effectiveness of universal vaccination and its effects on life expectancy. A few years later, in 1798, the Malthusian growth model was developed by Thomas Robert Malthus. In “An Essay on the Principle of Population” [5], he modeled population growth with the exponential equation

$$N(t) = N_0 e^{(rt)}, \quad (1)$$

where N_0 is the initial population, r is the growth rate and t is time. This is the solution to the linear ordinary differential equation

$$\frac{dN}{dt} = rN, \quad (2)$$

which simply states that the change in population is proportional to itself.

The Gompertz model was developed in 1825 by Benjamin Gompertz in “On the Nature of the Function Expressive of the Law of Human Mortality, and on a New Mode of Determining the Value of Life Contingencies” [6], and is given by

$$N(t) = N_0 e^{-ce^{at}-1}, \quad (3)$$

where a and c are constants. This model was constructed in an attempt to better understand human mortality. Gompertz was an actuary and his model was later used by insurance companies to estimate the cost of life insurance. His model confirmed that a person is more likely to succumb to death as they grow older. Between 1838 and 1847 the Belgian mathematician Pierre-Francois Verhulst developed the logistic equation to model population growth. The logistic equation is a nonlinear differential equation given by

$$\frac{dN}{dt} = rN - aN^2, \quad (4)$$

where N and t are population size and time respectively, and a is the density dependent crowding effect [7]. One can rewrite Eq. (4) as

$$\frac{dN}{dt} = rN \left(1 - \frac{N}{k}\right), \quad (5)$$

where k represents the maximum number of individuals that can be supported by an environment without destroying it. This equilibrium point at $N = k$ is the carrying capacity. At carrying capacity we have an unchanging population given by $\frac{dN}{dt} = 0$. When $N > k$, the population size will decline, approaching the carrying capacity from above, and when $N < k$, the population size will increase, approaching the carrying capacity from below.

In the early 1900s, approximately 100 years later, Anderson Gray McKendrick and William Ogilvy Kermack published “A Contribution to the Mathematical Theory of Epidemics” [8] in which

they developed the first compartmental model for infectious disease. This classical Susceptible-Infectious-Recovered, or *SIR* model is given as

$$\begin{aligned}\frac{dS}{dt} &= -\frac{\beta IS}{N}, \\ \frac{dI}{dt} &= \frac{\beta IS}{N} - \gamma I, \\ \frac{dR}{dt} &= \gamma I,\end{aligned}\tag{6}$$

where S is the number of susceptible individuals, I is the number of infectious individuals, and R is the number of recovered individuals in the population. By adding these three equations we obtain

$$\frac{dS}{dt} + \frac{dI}{dt} + \frac{dR}{dt} = 0,\tag{7}$$

which demonstrates that $S(t) + I(t) + R(t)$ is equal to a constant. This constant, N , is the total population size. Since R is decoupled from the S and I equations, the constant population means that we only need to study the first two of the three equations given by Eq. (6). We must also take note that the dynamics of the model depends on the basic reproduction number, R_0 , which provides the number of secondary infections that will be caused by a single infectious individual in an otherwise entirely susceptible population [9]. In the model given by Eq. (6), $R_0 = \frac{\beta}{\gamma}$. Over the past century since Kermack and McKendrick many researchers have used compartmental models to study infectious disease. The models have gotten more complicated, and accurate, by considering vitality rates, seasonality, age structure, etc., as well as the effect of control measures such as vaccine and quarantine. There are also stochastic models, network models, and spatial models, all of which are used to more accurately predict the spread of disease. These discoveries collectively are the basis of what is used by modern epidemiologists to understand and predict the outbreak, spread, and control of disease, including the recent COVID-19 pandemic.

2 Theory and Background

2.1 Compartmental models

Different compartmental models are used to study the outbreak, spread and control of a variety of infectious diseases. The more complicated the population of interest, the more factors and compartments that need to be accounted for in a model. In a compartmental model, the population could be experiencing a surge of immigrants or coupled completely with another population far away due to economic reasons. As discussed in the introduction, the simplest compartmental model divides the population into susceptible, infectious, and recovered groups. More complex models could also include exposed, hospitalized, deceased, or burial classes to name just a few. These models can easily be adapted to consider age structure, individuals with a compromised immune system, and many other features relevant to disease spread. To understand disease outbreak, spread, and extinction in a certain population, we need to know the rates at which all processes in the model occur (birth, death, transmission, recovery, etc.) The model includes these rates of change for each process which describes how individuals transition from one compartment to another. These mathematical models help us understand and investigate the spread of the disease as well as the implementation of strategies to control or contain the disease [10].



Figure 1: Schematic of the SIR compartmental model.

In the classic SIR model developed by Kermack and McKendrick [11], individuals in the population are divided into S , I , and R compartments representing susceptible, infectious, and recovered individuals respectively. Other similar models that are often used include the SIS , $SEIR$ and $SEIRS$ models, where the S , I , and R compartments are as defined in the SIR model, and the E compartment is defined as the exposed individuals (who are infected with the disease but are not yet infectious). More specifically, the different groups of individuals are defined as follows:

1. Susceptible (S): group of individuals who are vulnerable to the disease and may be infected if they come in contact with an infectious individual.
2. Exposed (E): group of individuals who are infected but are not yet infectious, and typically do not show any signs of the disease.
3. Infectious (I): group of infectious individuals who have the ability to transmit the disease to susceptible individuals.
4. Recovered (R): group of individuals who have recovered from the disease and are considered immune.

Details for three basic compartmental models of infectious diseases are discussed below.

2.1.1 Susceptible-Infectious-Recovered (SIR) Model:

The first epidemiological compartmental model due to Kermack and McKendrick [11] is the SIR model. This model is appropriate for any infectious disease in which permanent immunity is attained after recovery. Figure 1 shows a schematic outline of the compartment model with associated processes.

The governing equations for the SIR model with vital dynamics can be formulated as

$$\frac{dS}{dt} = \mu N - \frac{\beta IS}{N} - \mu S, \quad (8)$$

$$\frac{dI}{dt} = \frac{\beta IS}{N} - (\mu + \gamma)I, \quad (9)$$

$$\frac{dR}{dt} = \gamma I - \mu R, \quad (10)$$

where S , I , and R are the number of susceptible, infectious and recovered individuals respectively, $N = S + I + R$ is the total population size, μ is the birth and death rate, β is the contact rate,

and γ is the recovery rate. In these *SIR* equations, the μN term represents the number of healthy individuals born into the susceptible class, while the μS , μI , and μR terms give respectively the number of individuals leaving the *S*, *I*, and *R* classes due to natural death. Additionally, the $\frac{\beta IS}{N}$ term represents the number of susceptible individuals who become sick after contact with an infectious individual and move into the infectious class, while γI gives the number of individuals who transition from the infectious to the recovered compartment.

One can easily describe the *SIR* equations. For example, in Eq. (8), the rate of change of susceptible individuals in time is equal to the gain of individuals from healthy birth, the loss of individuals from the susceptible class to the infectious class due to infection, and a loss from natural death. Similarly, the rate of change of infectious individuals in time can be given as a gain of individuals due to infection, a loss of individuals from natural death, and a loss of individuals due to recovery. Lastly, the rate of change of recovered individuals in time is given by the gain due to recovery, and the loss of individuals due to natural death.

2.1.2 Susceptible-Infectious-Susceptible (*SIS*) Model

When the recovery does not give any immunity against the infection the model is known as the *SIS* model since recovered individuals immediately become susceptible to the disease again. Figure 2 shows a schematic outlining the compartmental model with associated processes. For this model, the governing equations become

$$\frac{dS}{dt} = \mu N - \frac{\beta IS}{N} - \mu S + \gamma I, \quad (11)$$

$$\frac{dI}{dt} = \frac{\beta IS}{N} - (\mu + \gamma)I, \quad (12)$$

where S and I are the number of susceptible and infectious individuals respectively, $N = S + I$ is the total population size, μ is the birth and death rate, β is the contact rate, and γ is the recovery rate. These equation can be described and analyzed in a similar manner to the *SIR* compartmental model above.

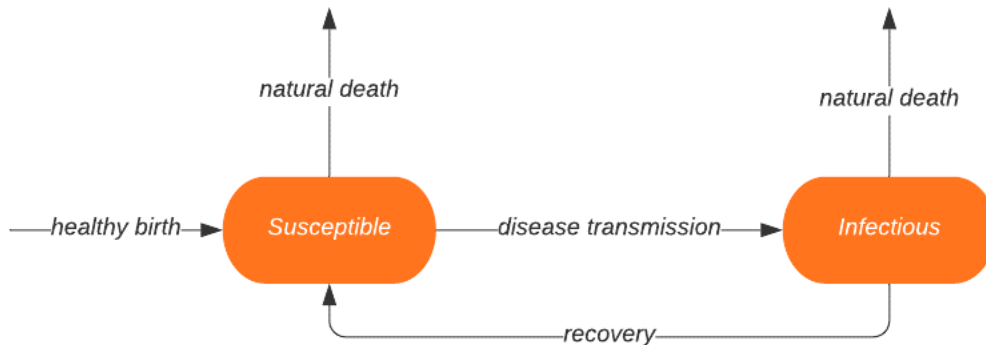


Figure 2: Schematic of the *SIS* compartmental model.

2.1.3 Susceptible-Exposed-Infectious-Recovered-Susceptible (*SEIRS*) Model

In the *SEIR* and *SEIRS* models the *S*, *I*, and *R* are the susceptible, infectious, and recovered respectively as we have seen above. The *E* compartment represents the exposed class. A susceptible individual who becomes infected with a disease is contained in the exposed class. During this latency period the individual, although infected, is not yet infectious (i.e., not yet able to transmit the disease to a susceptible individual). Eventually the individual moves to the infectious compartment and then recovers. The *SEIRS* system's compartmental model is shown in Figure 3.

The governing equations for the *SEIR* model can be formulated as:

$$\frac{dS}{dt} = \mu N - \frac{\beta IS}{N} - \mu S, \quad (13)$$

$$\frac{dE}{dt} = \frac{\beta IS}{N} - \mu E - \sigma E, \quad (14)$$

$$\frac{dI}{dt} = \sigma E - (\mu + \gamma)I, \quad (15)$$

$$\frac{dR}{dt} = \gamma I - \mu R, \quad (16)$$

where $S + E + I + R = N$, where N is the total population size, μ is the birth and death rate, β is the contact rate, γ is the recovery rate, and σ is the disease latency rate.

As mentioned, there are many other compartmental models that have been developed over the past century which include other groups and structures. Each compartmental model is used to describe and understand a certain type of disease outbreak and spread along with the effect of different control measures such as vaccine and quarantine policies. To mathematically model the dynamics of an infectious disease in a population, there are two broad approaches that one can consider. The classical compartmental approach, which was used by Kermack and McKendrick as well as many others over the years, is a deterministic approach. As we have seen, the model is

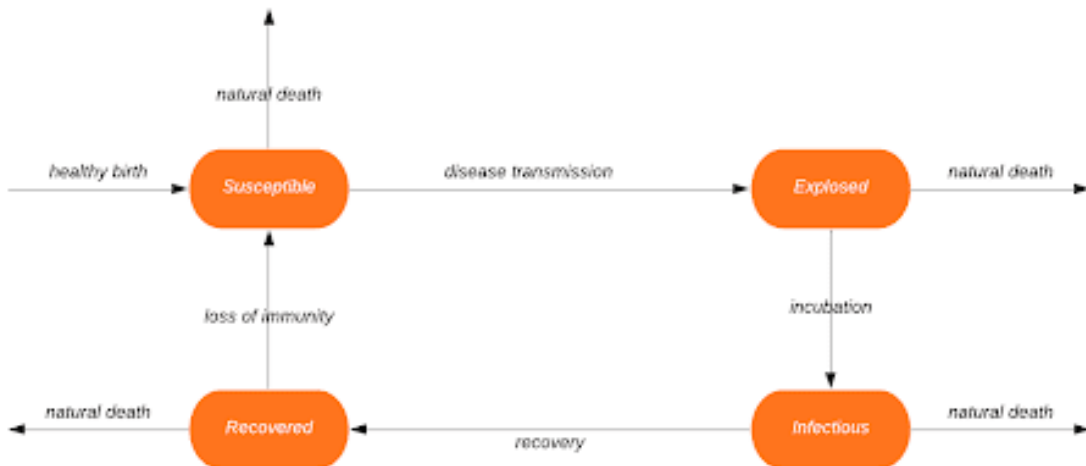


Figure 3: Schematic of the *SEIRS* compartmental model.

given by a set of ordinary differential equations whose solution determines exactly the state of the disease in time. In contrast to the deterministic approach, one can consider a stochastic approach which includes the noise or randomness that one finds in the real world.

2.2 Deterministic Models

In deterministic compartmental models a large population is divided into compartments. As discussed in the above example for the *SIR* model, the compartments are *S*, *I* and *R*. In this example, the mathematical model is formulated using ordinary differential equations. The population size in a compartment changes deterministically in time according to the transition rates and initial conditions. In short, for a prescribed set of parameter values and initial conditions the model always gives the same output no matter how many times we solve the equations. There is no randomness, and hence we have one output solution. These deterministic compartmental models often have two equilibria: an extinct state, in which there is no disease in the population, and an endemic state, in which the disease is maintained without any external forcing.

The transmission potential of a disease can be determined using the basic reproduction number, R_0 , which is the expected number of new infectious individuals generated by a single infectious individual in an entirely susceptible population [9]. The basic reproduction number tells us how quickly the disease could spread in a population. When $R_0 < 1$, the number of infectious individuals declines, and hence the disease will go extinct (possibly after a small outbreak). In this situation, the extinct state is a stable equilibrium while the endemic state is an unstable equilibrium. When $R_0 > 1$, the number of infectious individuals increases and the disease will be maintained in the population for a long period of time. In this scenario, the endemic state is stable while the extinct state is unstable. Usually in these types of models, $R_0 = 1$ serves as a threshold at which a transcritical bifurcation occurs. Because of the stability of the endemic state when $R_0 > 1$, in the deterministic approach there is no chance for the disease to go extinct [12].

2.2.1 Theoretical Analysis - An Example

As an example consider the following *SIS* epidemic system:

$$\frac{dS}{dt} = \mu N - \mu S - \frac{\beta IS}{N} + \gamma I, \quad (17)$$

$$\frac{dI}{dt} = \frac{\beta IS}{N} - \mu I - \gamma I, \quad (18)$$

where, *S* and *I* represent the susceptible and the infectious classes respectively, μ is the birth and death rate, β is the contact rate, and γ is the recovery rate. To find the equilibria points of such systems one must find the solutions to Eqs. (17) and (18) when they are set equal to zero. For the *SIS* compartmental model there are two equilibria states.

The first is $(S_0, I_0) = (N, 0)$, and is known as the disease free equilibrium state (DFE) or extinct state. In the DFE, all individuals of the population are in the susceptible class and the infectious class contains zero individuals from the population. The second equilibrium state is the endemic state and is given as $(S^*, I^*) = (\frac{N(\mu+\gamma)}{\beta}, (1 - \frac{\mu+\gamma}{\beta})N)$.

To determine the stability of the equilibrium points, we must construct the Jacobian matrix given as

$$J = \begin{bmatrix} \frac{\partial}{\partial S} f(S, I) & \frac{\partial}{\partial I} f(S, I) \\ \frac{\partial}{\partial S} g(S, I) & \frac{\partial}{\partial I} g(S, I) \end{bmatrix}, \quad (19)$$

where $f(S, I) = \mu N - \mu S - \frac{\beta IS}{N} + \gamma I$ and $g(S, I) = \frac{\beta IS}{N} - \mu I - \gamma I$ are the right-hand sides of Eqs. (17) and (18). Taking the appropriate partial derivatives gives

$$J = \begin{bmatrix} -\mu - \frac{\beta I}{N} & \frac{-\beta S}{N} + \gamma \\ \frac{\beta I}{N} & \frac{\beta S}{N} - \gamma - \mu \end{bmatrix}. \quad (20)$$

The Jacobian evaluated at the DFE is

$$J|_{(S_0, I_0)} = \begin{bmatrix} -\mu & -\beta + \gamma \\ 0 & \beta - \gamma - \mu \end{bmatrix}, \quad (21)$$

and the eigenvalues are given as $\lambda_1 = -\mu$ and $\lambda_2 = \beta - \gamma - \mu$. To stabilize the DFE, $\frac{\beta}{\gamma + \mu} < 1$ must be true. When $R_0 = \frac{\beta}{\gamma + \mu} < 1$, the DFE is stable, and when $R_0 = \frac{\beta}{\gamma + \mu} > 1$ the DFE is unstable. Similarly, one can evaluate the Jacobian at the endemic equilibrium, and by computing the eigenvalues it is easy to show that when $R_0 = \frac{\beta}{\gamma + \mu} < 1$ the endemic state is unstable, while when $R_0 = \frac{\beta}{\gamma + \mu} > 1$ the endemic state is stable. The two equilibrium states switch stability at $R_0 = 1$ denoting a transcritical bifurcation. As seen in this example the value and power of the basic reproductive number is a fundamental component of deterministic compartmental modeling [13].

The deterministic approach regards the time evolution as a continuous, wholly predictable process which is governed by a set of coupled ordinary differential equations. From the example above we see that when the endemic state is stable, extinction of the disease can essentially never be achieved since even after a perturbation away from the endemic state, the system will run back to the stable endemic equilibrium. However, one often sees local extinction events in data collected in the real world. To properly capture the extinction events, one must include stochasticity or random noise in the model. In contrast to the deterministic approach, the stochastic approach regards the time evolution as a type of random-walk process, which typically is described using a Langevin equation (for external noise) or a master equation (for internal noise) [12, 14].

3 Stochastic Models

Historically, we see that disease outbreaks often do go extinct locally. In order to capture these extinction events mathematically, we must use a stochastic model that includes the randomness or noise in the system. In particular, in this work we will capture the effect of internal demographic noise with the master equation. The master equation gives the probability of the system having a particular number of susceptible, infectious, etc. individuals at any instant in time. The internal noise can lead to a rare, large fluctuation that causes the disease to “escape” from the deterministically stable endemic state and go to the extinct state [12, 14–20]. For the simplest of problems it is possible to perform theoretical analysis to solve the master equation. However, in many instances, one must simulate the stochastic solutions numerically to understand the system’s behavior. In the following sections we present an overview of the theoretical and numerical tools used to understand epidemic models that include internal noise.

3.1 Master Equation and Internal Noise

As we have seen, deterministic compartment models have equilibrium points that can be analyzed to see when they are stable or unstable. On the other hand, stochastic systems, by nature, are

different. In reality, many systems have equilibria that are considered to be metastable [14], meaning that the stochastic system fluctuates about the deterministic steady-state for a long period of time, but can ultimately escape from the metastable state and transition to another metastable state or an absorbing state.

To analyze stochastic systems similar to the ones constructed from the compartmental models above, we assume the discrete transitions in a large enough population are short and independent in time. Therefore, the system is a Markov process and the evolution of the system is described by the master equation

$$\frac{\partial \rho(X, t)}{\partial t} = \sum_r [W_r(X - r)\rho(X - r, t) - W_r(X)\rho(X, t)], \quad (22)$$

where X is a state of individuals in a population, $\rho(X, t)$ is the probability of finding X individuals at time t , and $W_r(X)$ is the transition rate from X to $X + r$, and r may be a positive or a negative integer increment. As can be observed, the first term in the master equation is the increase in X from the $X - r$ state, while the second term is the decrease of X to the $X + r$ or $X - r$ states.

Assuming a large enough population, a WKB approach can be used to approximate the master equation [12]. Again, assuming a large population size, the time for disease extinction can be very long and is determined by the tail of the quasi-stationary probability density function (PDF) where $\frac{\partial \rho}{\partial t} \approx 0$ and we can set the master equation equal to zero as shown by

$$0 = \sum_r [W_r(X - r)\rho(X - r, t) - W_r(X)\rho(X, t)]. \quad (23)$$

Now we will scale X by N , the usual population size in the metastable state. Using $x = \frac{X}{N}$, the transition rate $W_r(X) = W_r(Nx)$ and when Taylor expanded in N the rate becomes

$$W_r(Nx) = Nw_r(x) + u_r(x) + \mathcal{O}(1/N), \quad (24)$$

where w_r and u_r are $\mathcal{O}(1)$. We can also rewrite the scaled probability as

$$\rho(X) \equiv \rho(Nx) = \pi(x). \quad (25)$$

Then the scaled master equation becomes

$$0 = \sum_r [w_r(x - \frac{r}{N})\pi(x - \frac{r}{N}) - w_r(x)\pi(x)]. \quad (26)$$

To apply the WKB approximation we assume that $N \gg 1$ and that

$$\pi(x) = A(x)e^{-NS(x)(1+\mathcal{O}(1/N))}, \quad (27)$$

and after substituting the WKB ansatz into the master equation we obtain a Hamilton-Jacobi equation with Hamiltonian

$$\mathcal{H}(x, \lambda) = \sum_r w_r(x)e^{(r\lambda)-1} = 0, \quad \lambda = \frac{\partial \mathcal{S}}{\partial x}. \quad (28)$$

Hamilton's Equations are then given by

$$\begin{aligned}\dot{x} &= \frac{\partial \mathcal{H}}{\partial \lambda} = \sum_r r w_r(x) e^{(r\lambda)}, \\ \dot{\lambda} &= -\frac{\partial \mathcal{H}}{\partial x} = -\sum_r e^{(r\lambda-1)} \frac{\partial w_r(x)}{\partial x}.\end{aligned}\tag{29}$$

For single-step processes such as found in epidemic models, the mean time to extinction can be approximated [12] by

$$\tau = B e^{N \mathcal{S}_{opt}},\tag{30}$$

where B is a prefactor that depends on the system's parameters and the population size,

$$\mathcal{S}_{opt} = \int^x \lambda_{opt}(x) dx,\tag{31}$$

with limits of integration that depend on the equilibrium points, and

$$\lambda_{opt}(x) = -\ln \left(\frac{w_{+1}(x)}{w_{-1}(x)} \right).\tag{32}$$

3.2 Gillespie Algorithm

To generate a solution of a stochastic equation where the noise is internal to the system we use the Gillespie algorithm or Doob-Gillespie algorithm. The algorithm is a type of Monte Carlo method popularized by Daniel T. Gillespie [21] as a method for simulating chemical reactions based on molecular collisions. The results of a Gillespie simulation is a stochastic trajectory that correctly captures the probability function that solves the master equation. Therefore the Gillespie algorithm has become an integral part of understanding and analyzing disease spread where molecular collisions are replaced by individual events associated with disease outbreak and spread [12].

The Gillespie algorithm can be described using the following steps:

1. Initialization and identification of reaction states and rates of change. Let $\mathbf{x} = (x_1, \dots, x_n)^T$ represent the compartments of a system, where x_i is the number of individuals in compartment x_i at time t . Set the time and reaction counter to zero. Initialize uniform random number generators for the event and the time the event occurs.
2. Calculation of transition rates. For a given state \mathbf{x} , the transition rates are given as $a_i(\mathbf{x})$ for $i = 1 \dots l$, where l is the number of transitions. Thus the sum of all transition rates is given by $a_0 = \sum_{i=1}^l a_i(\mathbf{x})$.
3. Generation of random numbers r_1 and r_2 and calculation of τ . One simulates the time τ until the next transition by drawing from an exponential distribution with mean $1/a_0$. This is equivalent to drawing a random number r_1 uniformly on $(0, 1)$ and computing $\tau = (1/a_0) \ln(1/r_1)$. During each random time step exactly one event occurs. The probability of any particular event taking place is equal to its own transition rate divided by the sum of all transition rates $a_i(\mathbf{x})/a_0$. A second random number r_2 is drawn uniformly on $(0, 1)$, and

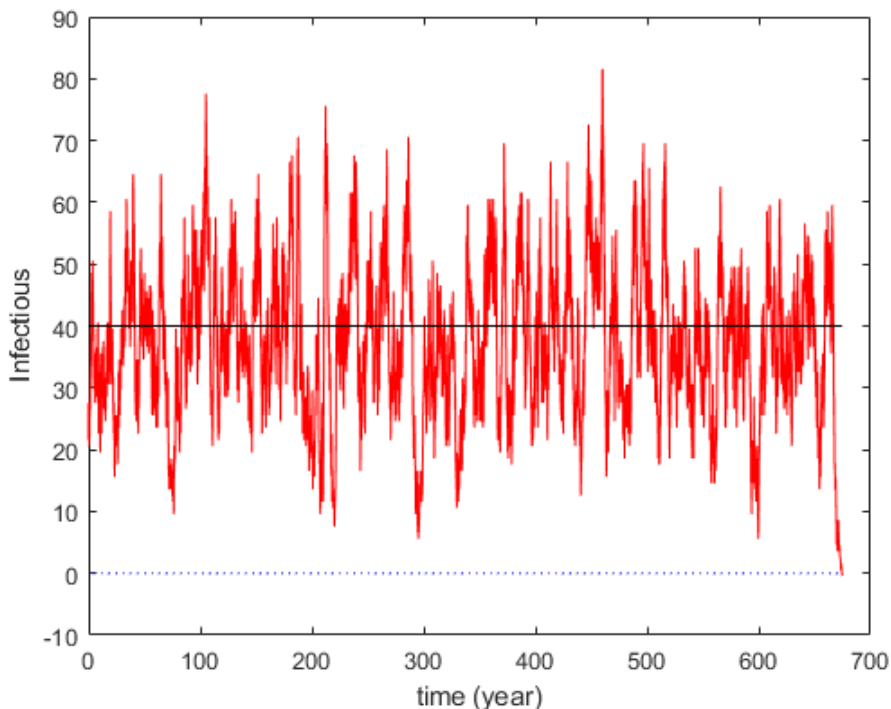


Figure 4: Infectious individuals in time for the SIS model. The red curve is a single stochastic trajectory showing fluctuations about the deterministically stable endemic state (black line) before the eventual extinction. The parameter values are: $\mu = 0.9$, $\gamma = 0.1$, $\beta = 1.4$, and $N = 100$.

it is used to determine the transition event that occurs. If $0 < r_2 < a_1(\mathbf{x})/a_0$, then the first transition occurs; if $a_1(\mathbf{x})/a_0 < r_2 < (a_1(\mathbf{x}) + a_2(\mathbf{x}))/a_0$, then the second transition occurs, and so on.

4. Iteration of τ and updating the individuals in each compartment. The process repeats until extinction occurs or the simulation time limit is reached [12].

Figure 4 shows the number of infectious individuals in time for a single realization of the stochastic *SIS* model found using the Gillespie algorithm. One sees the fluctuations around the deterministically stable endemic equilibrium until eventually the disease goes extinct.

3.3 Complex Example: The Ebola Model

We now demonstrate the application of these stochastic modeling techniques to an Ebola virus disease (EVD) model based on extending an *SEIR* model, and presented by Garrett T. Nieddu, et al. in “Extinction Pathways and Outbreak Vulnerability in a Stochastic Ebola Model” [19]. EVD was first discovered in Zaire (currently the Democratic Republic of Congo) near the Ebola river from which the disease was named. EVD is an infectious zoonosis, a disease found in animals that can be transmitted to humans with symptoms that may or may not affect the animal host. For example, EVD is very deadly in apes yet infected bats show no symptoms. Although it is

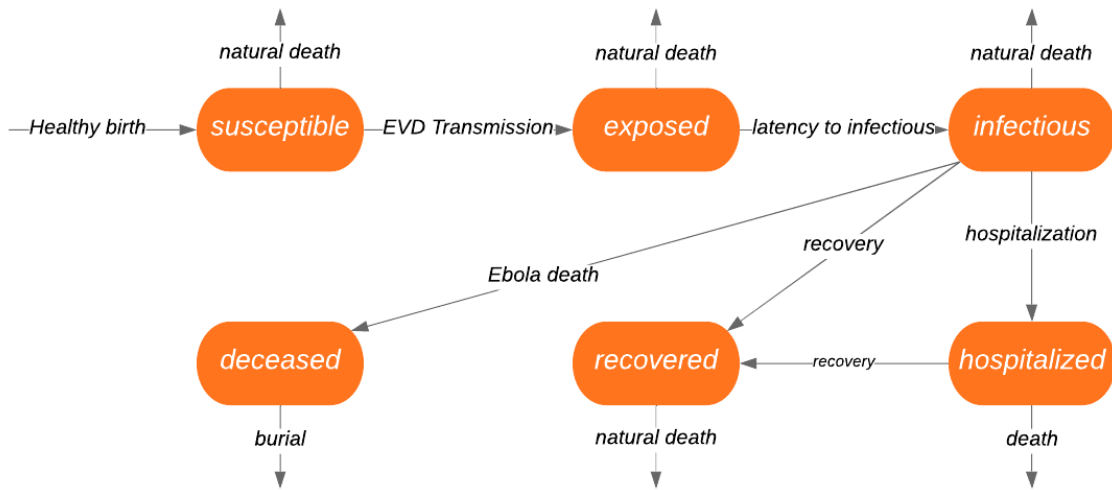


Figure 5: Schematic of the Ebola Virus Disease (EVD) compartmental model.

relatively difficult for EVD to invade human populations, there have been many spillover events, when the disease is transferred from the animal reservoir into the human population, by contact with bodily fluid. The CDC in the United States of America estimates that more than 28 thousand infections and 11 thousand deaths occurred in the most recent West African epidemic. The sporadic appearances and disappearances of the disease in the human population is more evidence that the disease is maintained in animal populations. This implies that EVD must be analyzed under the context of random interactions between the infected hosts that serve as a reservoir of disease and human populations [19].

Given the incubation time of the disease which ranges from 7-21 days, an approach based on the susceptible-exposed-infectious-recovered (*SEIR*) model is appropriate. A deterministic model could be used, but to properly capture the random interactions between individuals, and to capture the stochastic events in which disease from the reservoir enters the population, one should use a stochastic version of the model. The stochastic EVD model presented in Ref. [19] accounts for the random events and interactions taking place within the population, including birth and death, and infection of susceptibles, but also includes hospitalization and burial. Burials in particular are quite important as this was a large source of new infections during the recent West African EVD outbreak. A complete flow chart of all the possible interactions accounted for in this model is presented in Figure 5. Although this type of model has been used in previous EVD studies, the random contact with the animal reservoir had never been accounted for. Table 1 lists the events in the stochastic EVD model along with their associated rates, while Table 2 lists the various parameter values.

By observing the transition events of the stochastic EVD in Table 1, one can see that there are two distinct ways an individual might become infected. The infection may come from a human interaction in which a susceptible individual comes into contact with an infectious, hospitalized, or deceased individual, or the infection may be transmitted by a susceptible coming into contact with

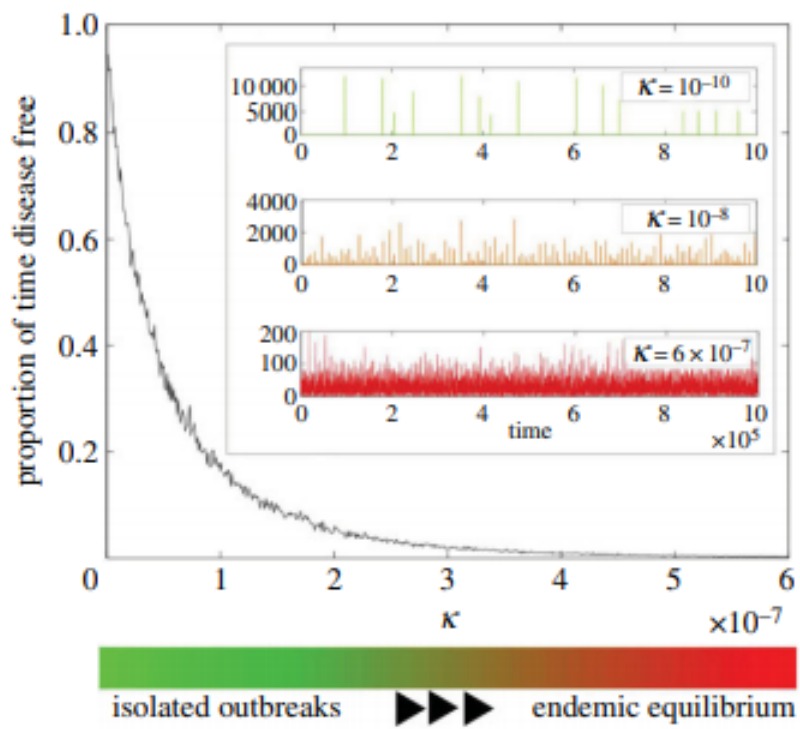


Figure 6: Outbreak vulnerability in the EVD model showing different outbreak scenarios. The figure is taken from Ref. [19].

Event	Transition	Rate
healthy birth	$\phi \rightarrow S$	μN
EVD transition (human)	$S \rightarrow E$	$(\beta_i I + \beta_d D + \beta_h H)(\frac{S}{N})$
EVD transition (animal)	$S \rightarrow E$	κS
latency to infectious	$E \rightarrow I$	σE
recovery	$I \rightarrow R$	$\gamma_{ir} I$
EVD death	$I \rightarrow D$	$\mu_e I$
hospitalization	$I \rightarrow H$	τI
burial	$D \rightarrow \phi$	δD
death from hospital	$H \rightarrow \phi$	$\mu_e H$
recovery from hospital	$H \rightarrow R$	$\gamma_{hr} H$
natural death	$S, E, I, D, H, R \rightarrow \phi$	$\mu(S, E, I, D, H, R)$

Table 1: Events, transitions, and rates in the stochastic EVD model.

the disease reservoir with reservoir transmission rate κS . The addition of the κS term in this model is critical in the analysis to understand the behaviour of the disease spread in the population. The disease state of the population will be directly affected by the strength of the coupling with the animal reservoir. The stronger the coupling, the more frequent new infections appear. For smaller values of κ , disease outbreaks will be less frequent, while for large values, the disease may become endemic in the population. The effects of κ can be observed in Figure 6 which shows the different types of outbreak states that can occur when the animal reservoir transmission rate is varied. The top time series in the inset shows the number of infectious individuals over time when $\kappa = 10^{-10}$, and we see that the population with these parameters is mostly disease free while experiencing rare outbreak events. This scenario is referred to as the rare outbreak zone (ROZ). In the middle time series when $\kappa = 10^{-8}$, the population is experiencing frequent outbreaks between periods of disease

Description	Parameter	Value
1/host life span (and birth rate)	μ	$0.00005d^{-1}$
contact rate for infectious	β_i	$0.5d^{-1}$
contact rate for deceased	β_d	$0.6d^{-1}$
contact rate for hospitalized	β_h	$0.00016d^{-1}$
1/latency period	σ	$0.1d^{-1}$
1/recovery period (no hospital)	γ_{ir}	$0.07d^{-1}$
death rate from EVD	μ_e	$0.12d^{-1}$
1/mean time to hospitalization	τ	$0.2d^{-1}$
1/burial time	δ	$0.33d^{-1}$
1/recovery period (hospital)	γ_{hr}	$0.10d^{-1}$
reservoir transmission	κ	$5.0 \times 10^{-9}d^{-1}$

Table 2: Numerical values for the parameters in the EVD model.

Event	Transition	Rate
healthy birth	$\phi \rightarrow S$	μN
transition (human)	$S \rightarrow I$	$(\frac{\beta IS}{N})$
transition (reservoir)	$S \rightarrow I$	κS
recovery	$I \rightarrow S$	γI
natural death	$(S, I) \rightarrow \phi$	$\mu(N, I)$

Table 3: Events, transitions, and rates in the stochastic $SIS\kappa$ model.

extinction. This scenario will be referred to as the frequent outbreak zone (FOZ). The bottom time series for $\kappa = 6.0 \times 10^{-7}$ shows a population that is never free of disease and is in the perpetually endemic zone (PEZ) [14].

It is worth noting that this EVD model is quite complex, and therefore the analysis performed in Ref. [19] is almost entirely numerical. To better understand the outbreak vulnerability results of the EVD model, we consider a simplified version, namely a Susceptible-Infectious-Susceptible- κ ($SIS\kappa$) model that includes reservoir transmission of disease for the SIS population model. In addition, we will consider the effect of vaccination for the $SIS\kappa$ model.

4 Stochastic Zoonotic SIS Models

4.1 Susceptible-Infectious-Susceptible- κ ($SIS\kappa$) Model

In a Susceptible-Infectious-Susceptible- κ ($SIS\kappa$) compartmental model the S and I stand respectively for susceptible and infectious individuals, just as in the other compartmental models discussed previously. In this model the κ term is introduced to account for disease introduction from an external zoonotic source, adding a generic infection event. The transition rates β , γ , and μ remain contact rate, recovery rate, and birth/death rate respectively. The additional κ rate is the transmission rate between the population and the reservoir. Table 3 describes all the transition rates for this model while Figure 7 shows the relationship between the different compartments and the associated transition events.

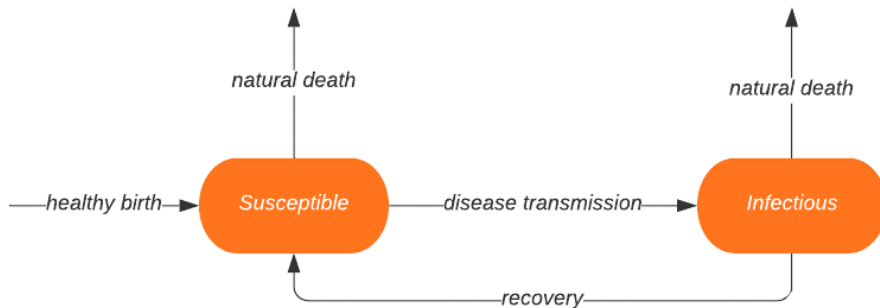


Figure 7: Schematic of the $SIS\kappa$ compartmental model.

The governing equations of the system are given by

$$\begin{aligned}\frac{dS}{dt} &= \mu N - \mu S - \frac{\beta IS}{N} - \kappa S + \gamma I, \\ \frac{dI}{dt} &= \frac{\beta IS}{N} + \kappa S - (\mu + \gamma)I.\end{aligned}\tag{33}$$

Assuming a constant population so that $N = S + I$, the two-dimensional system in S and I can be reduced to a one-dimensional system in I that is given by

$$\frac{dI}{dt} = (\beta I + \kappa N) - \left(\frac{\beta I^2}{N} + (\kappa + \mu + \gamma)I \right).\tag{34}$$

Recall that the classic SIS compartmental model discussed previously had two distinct equilibrium points, one for the disease endemic state and another for the disease free state. In the $SIS\kappa$ compartmental model, the addition of the κ term effectively eliminates the disease extinction state. There is still however a disease endemic state given by

$$I^* = N \left[\frac{\beta - \gamma - \kappa - \mu + \sqrt{(\beta - \gamma - \kappa - \mu)^2 + 4k\beta}}{2\beta} \right]\tag{35}$$

Since the one-dimensional model of disease transfer is assumed to be a Markov processes, the master equation can be used to understand the stochastic model. To construct the master equation we begin by rewriting it in terms of its different structures, namely the growth and decay rates of the infectious class. The $SIS\kappa$ system has a master equation given as

$$\frac{dP_I}{dt} = \lambda(I-1)P_{I-1} - \lambda(I)P_I + \delta(I+1)P_{I+1} - \delta(I)P_I,\tag{36}$$

where P_I denotes the probability of having I individuals at time t , and where the growth term $\lambda(I)$, and the decay term $\delta(I)$, are defined in Eq. (34) as

$$\lambda(I) = (\beta I + \kappa N), \quad \text{and} \quad \delta(I) = \frac{\beta I^2}{N} + (\kappa + \mu + \gamma)I.\tag{37}$$

Thus the master equation of the system becomes

$$\begin{aligned}\frac{dP_I}{dt} &= [\beta(I-1) + \kappa N] P_{(I-1)} \\ &\quad - \left[\beta I + \kappa N + \frac{\beta I^2}{N} + (\kappa + \mu + \gamma)I \right] P_{(I)} \\ &\quad + \left[\frac{\beta(I+1)^2}{N} + (\kappa + \mu + \gamma)(I+1) \right] P_{(I+1)}.\end{aligned}\tag{38}$$

A master equation of this form has a stationary solution that can be found analytically as [22]

$$\rho(I) = \pi_0 \prod_{n=1}^I \frac{\lambda(n-1)}{\delta(n)},\tag{39}$$

where π_0 is a normalization factor and which for our choice of λ and δ can be rewritten as

$$\rho(I) = \frac{\pi_0 N^I}{\Gamma(I+1)} \cdot \frac{\Gamma\left(\frac{N\kappa}{\beta} + I\right)}{\Gamma\left(\frac{N\kappa}{\beta}\right)} \cdot \frac{\Gamma\left(\frac{(\mu+\gamma+\kappa)N}{\beta} + 1\right)}{\Gamma\left(\frac{(\mu+\gamma+\kappa)N}{\beta} + 1 + I\right)}, \quad (40)$$

where $\Gamma(x)$ denotes the Gamma function. The mean value of this probability density function (PDF) is given by I^* , and by evaluating the above equation for a specified set of parameter values, one can find the probability of having I infectious individuals in the population [14].

Figures 8 and 9 represent respectively nine PDFs and stochastic realizations of the stochastic $SIS\kappa$ using parameter values $(\mu, \gamma, \beta) = (5.0 \times 10^{-5}, 0.33, 0.1)$ and varying N and κ values in each of the nine sub-plots. In Figure 9, observe that the blue graphs show dynamics associated with the frequent outbreak zone (FOZ), so that there are many extinction and outbreak event with little time spent disease free. The red graphs represent dynamics associated with the perpetually endemic zone (PEZ), so that the disease is endemic. Lastly, the green graphs represent dynamics in the rare outbreak zone (ROZ), where the population experiences rare outbreaks with plenty of disease free time [14]. Looking back to Figure 8 we see that the PDFs have different shape corresponding to whether they lie in the FOZ, PEZ, or ROZ.

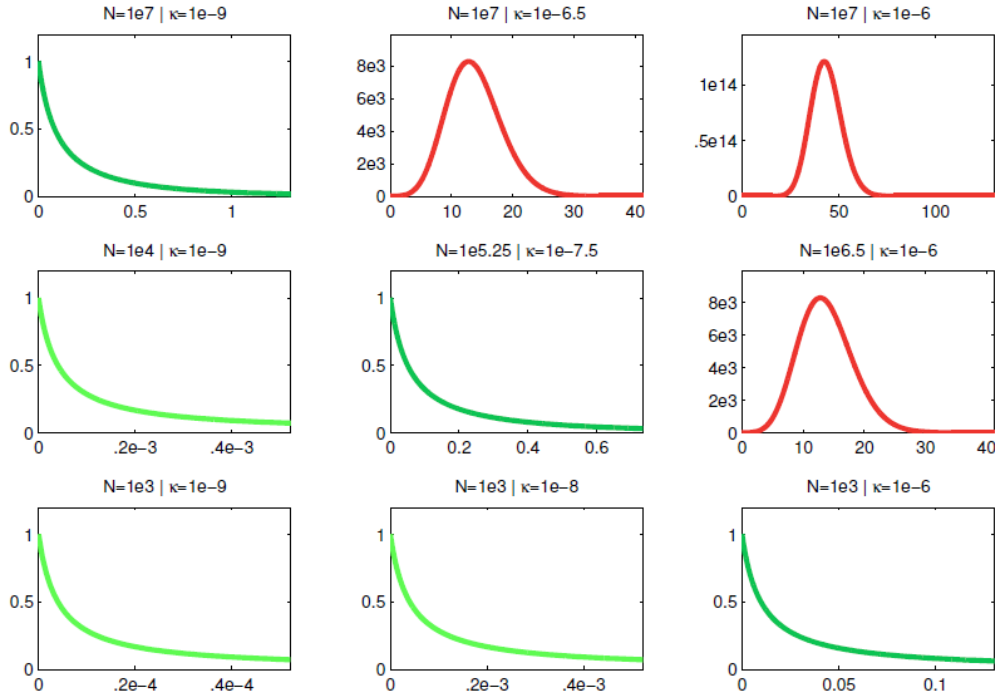
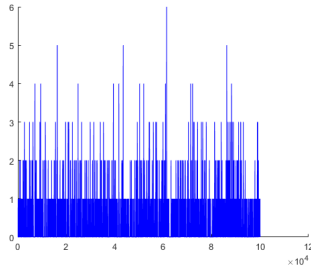
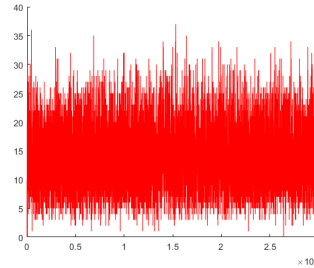


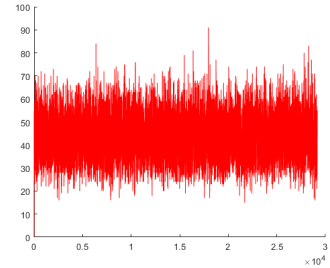
Figure 8: Probability density functions of the stochastic $SIS\kappa$ model for a range of N and κ values. The figure is taken from Ref. [14]. Parameter values are $\beta = 0.1$, $\gamma = 0.33$, and $\mu = 5.0 \times 10^{-5}$.



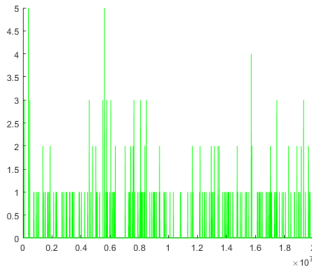
(a) $N=1e7, \kappa=1e-9$



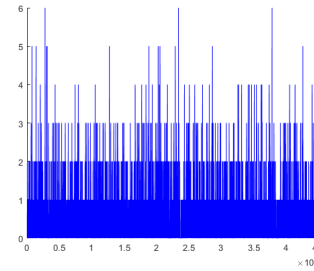
(b) $N=1e7, \kappa=1e-6.5$



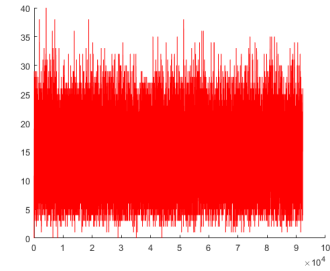
(c) $N=1e7, \kappa=1e-6$



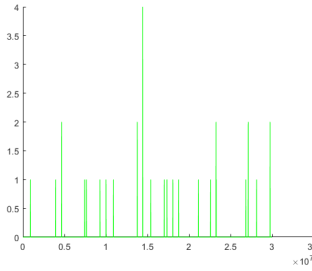
(d) $N=1e4, \kappa=1e-9$



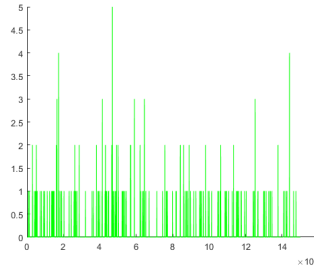
(e) $N=1e5.25, \kappa=1e-7.5$



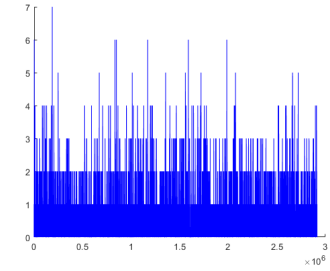
(f) $N=1e6.5, \kappa=1e-6$



(g) $N=1e3, \kappa=1e-9$



(h) $N=1e3, \kappa=1e-8$



(i) $N=1e3, \kappa=1e-6$

Figure 9: Stochastic realizations of the $SIS\kappa$ model for a range of N and κ values. Parameter values are $\beta = 0.1$, $\gamma = 0.33$, and $\mu = 5.0 \times 10^{-5}$.

4.2 Susceptible-Infectious-Susceptible- κ ($SIS\kappa$) Model with Vaccine

We now extend the stochastic $SIS\kappa$ model to consider the effect of vaccine on the disease dynamics. We add a vaccine V compartment which contains individuals who were vaccinated and therefore are no longer susceptible. In this model, c represents the vaccination rate. All events and associated transitions and rates are shown in Table 4, while Figure 10 shows a schematic of the stochastic $SIS\kappa$ model with vaccination ($SIS\kappa - V$).

Event	Transition	Rate
healthy birth	$\phi \rightarrow S$	μN
natural death	$S, I, V \rightarrow \phi$	$\mu(S, I, V)$
transition	$S \rightarrow I$	$\frac{\beta IS}{N} + \kappa S$
recovery	$I \rightarrow S$	γI
vaccination	$S \rightarrow V$	cS

Table 4: Rates and events in $SIS\kappa - V$ model.

The governing equations of the $SIS\kappa - V$ model are given by

$$\begin{aligned}
 \frac{dS}{dt} &= \mu N - \mu S - \frac{\beta IS}{N} + \gamma I - cS - \kappa S, \\
 \frac{dI}{dt} &= \frac{\beta IS}{N} + \kappa S - (\mu + \gamma)I, \\
 \frac{dV}{dt} &= cS - \mu V.
 \end{aligned} \tag{41}$$

As before, we assume a constant population so that $N = S + I + V$. The endemic equilibrium is

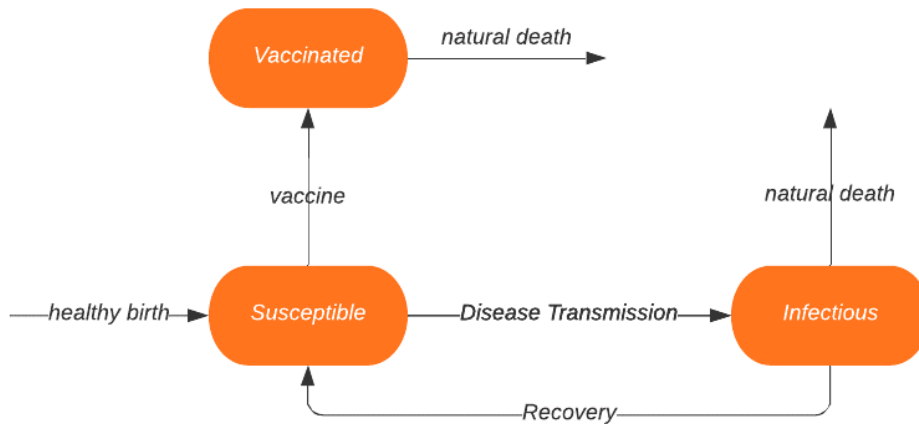


Figure 10: Schematic of the $SIS\kappa - V$ compartmental model.

given as

$$I^* = (-[\mu^2 N + cN\mu + \kappa N\mu + \mu N\gamma + cN\gamma - \beta\mu N] + \sqrt{(\mu^2 N + cN\mu + \kappa N\mu + \mu N\gamma + cN\gamma - \beta\mu N)^2 + 4\beta\mu^2 \kappa N^2}) / 2\beta\mu. \quad (42)$$

Because of the additional complexity from the vaccine class, unlike the $SIS\kappa$ model, we will not be able to analytically find a stationary solution to the master equation. Nevertheless, we can numerically solve the system to understand the changes in dynamics due to varying levels of vaccination.

Figure 11 shows the effects of varying the amount of vaccination using the same parameter values used in the non-vaccine model (Figure 9). Each sub-figure of Figure 11 shows nine stochastic realizations for different N and κ values, with each sub-figure showing results for different values of c ranging from $c = 10\%$ to $c = 90\%$ increasing in uniform increments of 10% from top to bottom, and left to right. In all realizations one can observe a difference in the population dynamics with the vaccine control added to the $SIS\kappa$ compartmental model.

In the realizations across the diagonal which showed a FOZ previously, we now have comparable behavior to the ROZ realizations. In sub-figure (a), the realizations can clearly be now classified as the ROZ, with more disease extinction events clearly visible in all realizations to no outbreaks at all in the realization corresponding to $c = 90\%$. In sub-figure (e) one can see that there are far fewer outbreaks compared to the scenario with the same parameters in the $SIS\kappa$ model without vaccination. For sub-figure (i) one can observe that the difference is not as drastic as in the others along the diagonal. The population is still in the FOZ but with an average of only one infected person per outbreak, an improvement is seen.

In the realizations that were previously in the PEZ we can observe sub-figures (b), (c) and (f) to see the effect of vaccine. One sees that vaccine has dramatically decreased the number of infected individuals in the population as time evolves. The vaccine has moved these populations from the PEZ to the FOZ. In the bottom left corner are realizations that were all previously in the ROZ. One can observe in sub-figure (h) that not much has changed to the population dynamics with c values between 10% and 50% . On the other hand, when c is between 60% and 90% one sees that the number of outbreaks has decreased dramatically to an almost constant disease free state. In sub-figures (d) and (g) we observe a similar effect to the population dynamics where there are rare outbreaks, if there are any at all, and the number of infections does not pass two infectious individuals. We can confidently say that the vaccine has positively improved the situation of the previously ROZ to one with essentially no outbreaks at all.

Overall, the effects of the vaccine to the initial $SIS\kappa$ compartmental model are clearly visible in all realizations with c ranging from 10% to 90% . The effects are all positive with respect to the population dynamics. Most realizations from the $SIS\kappa$ vaccine group could be classified as having less severe outbreak vulnerability zones as compared to the non-vaccine case. In general, scenarios that were in the PEZ become FOZ, FOZ scenarios become ROZ, and ROZ scenarios move to disease free states. Figure 12 is similar to Figure 11 but with smaller rates of vaccination. Here the vaccine rate, c , ranges from 1% to 9% . One can observe that the effects are almost mirrored from Figure 11. We have similar effects on a smaller scale with no major differences. Figure 13 for vaccine rates ranging from 91% to 99% also shows similar results to those seen in Figure 11. Here the scale of change in the the dynamics of the population is steeper and sharper. In the previously FOZ scenarios, the decrease in the number of infectious individuals in the population is dramatic, and the disease has very rapidly approached extinction.

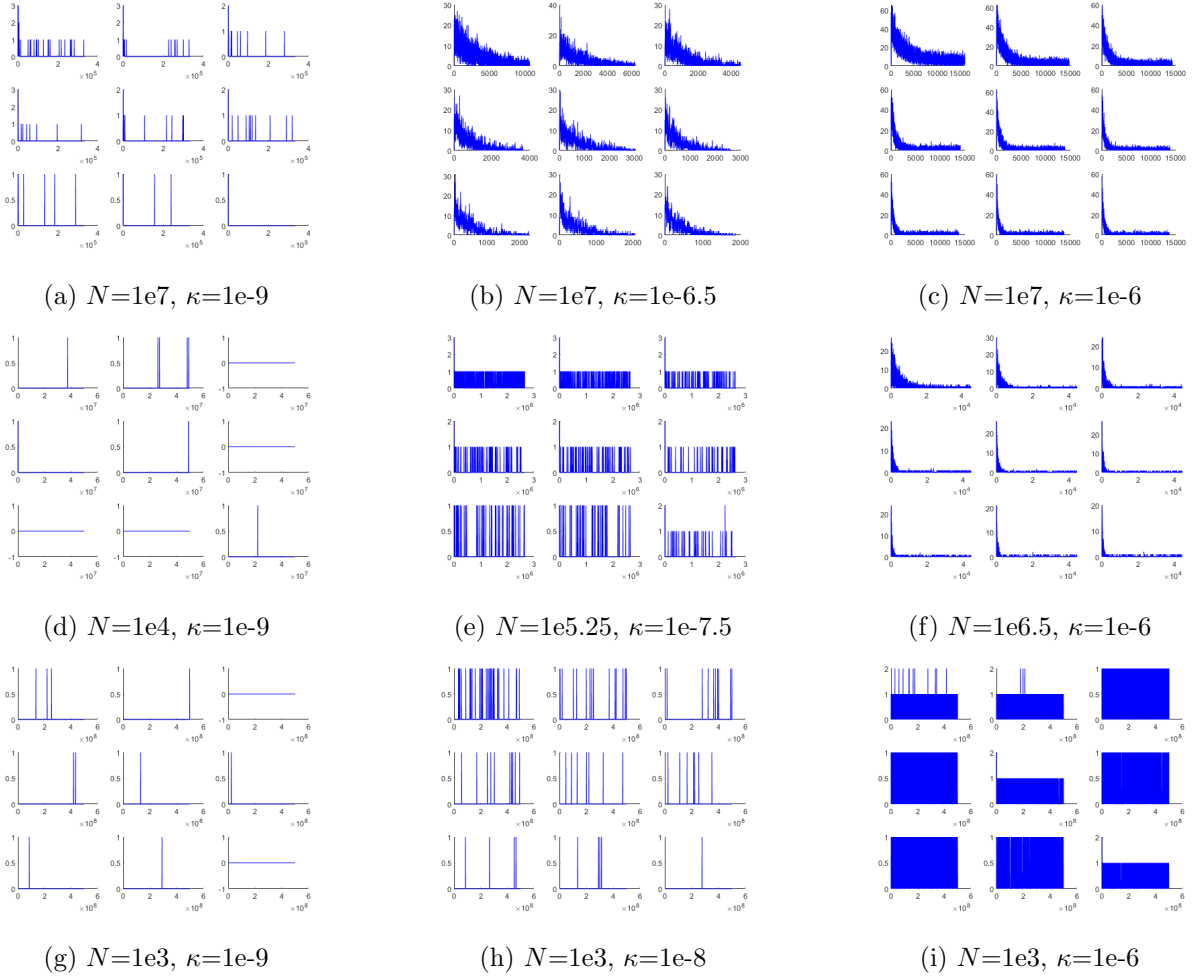


Figure 11: Stochastic $SIS\kappa - V$ realizations with 10% to 90% vaccination rates for varying N and κ values. Each sub-figure shows nine stochastic realizations with each sub-figure showing results for different values of c ranging from $c = 10\%$ to $c = 90\%$ increasing in uniform increments of size 10% from top to bottom, and left to right.

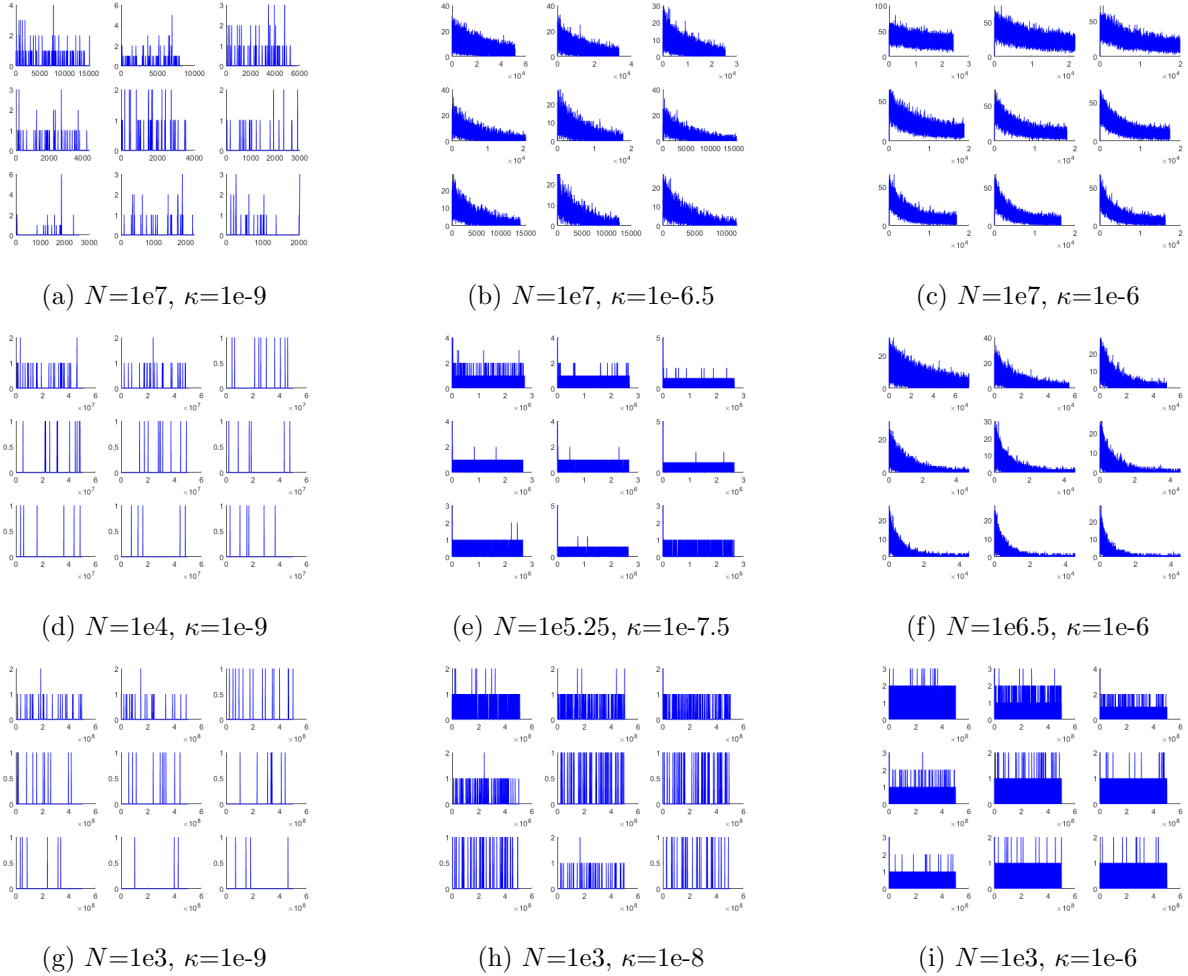
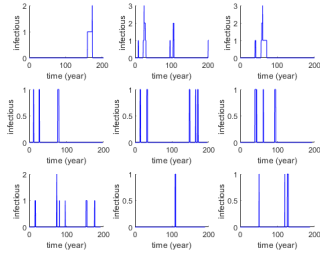
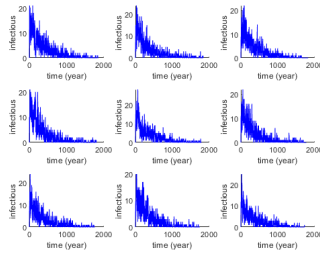


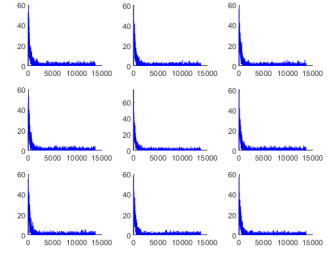
Figure 12: Stochastic $SIS\kappa - V$ realizations with 1% to 9% vaccination rates for varying N and κ values. Each sub-figure shows nine stochastic realizations with each sub-figure showing results for different values of c ranging from $c = 1\%$ to $c = 9\%$ increasing in uniform increments of size 1% from top to bottom, and left to right.



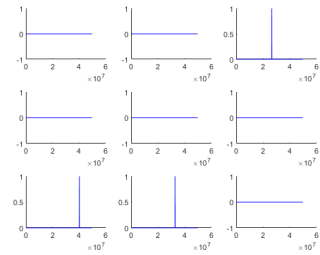
(a) $N=1e7, \kappa=1e-9$



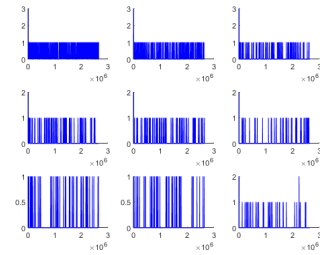
(b) $N=1e7, \kappa=1e-6.5$



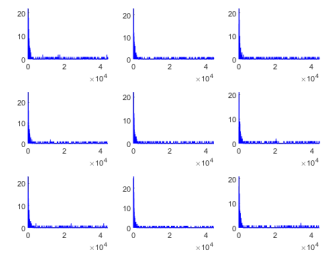
(c) $N=1e7, \kappa=1e-6$



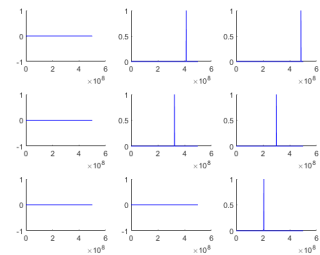
(d) $N=1e4, \kappa=1e-9$



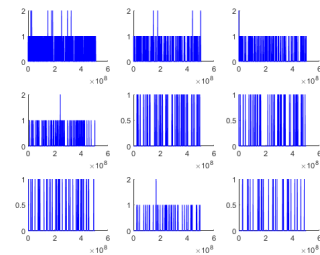
(e) $N=1e5.25, \kappa=1e-7.5$



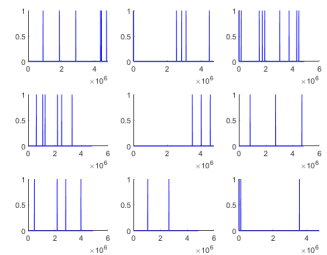
(f) $N=1e6.5, \kappa=1e-6$



(g) $N=1e3, \kappa=1e-9$



(h) $N=1e3, \kappa=1e-8$



(i) $N=1e3, \kappa=1e-6$

Figure 13: Stochastic $SIS\kappa - V$ realizations with 91% to 99% vaccination rates for varying N and κ values. Each sub-figure shows nine stochastic realizations with each sub-figure showing results for different values of c ranging from $c = 91\%$ to $c = 99\%$ increasing in uniform increments of size 1% from top to bottom, and left to right.

5 Summary

Epidemiology is an integral field of science in a modern day world where disease outbreaks have become increasingly more common in human populations. Understanding and analyzing the behavior and the spread of these diseases is an essential task in driving them to extinction. In this thesis, we have provided an overview of different epidemiological compartmental models, and we have discussed both deterministic and stochastic versions. By implementing the the Gillespie algorithm, we are able to simulate stochastic solutions where the stochasticity is due to the internal noise in the system. Specifically we considered stochastic versions of zoonotic models including complex models needed for Ebola Virus Disease modeling as well as simplified models that enable theoretical analysis. Lastly, we considered the effect of vaccine on outbreak vulnerability for a type of zoonotic model. In comparing the $SIS\kappa$ and $SIS\kappa - V$ with vaccination models, one can observe that vaccine leads to beneficial changes in the population dynamics and vulnerability to disease outbreak. The positive changes include both a decrease in the number of infectious individuals during an outbreak as well as the frequency of outbreaks.

6 Bibliography

References

- [1] A. Aschengrau and G. R. Seage, Essentials of epidemiology in public health. Jones & Bartlett Publishers, 2013.
- [2] R. C. Dicker, F. Coronado, D. Koo, and R. G. Parrish, “Principles of epidemiology in public health practice; an introduction to applied epidemiology and biostatistics,” 2006.
- [3] J. Graunt, Natural and political observations mentioned in a following index, and made upon the Bills of Mortality. 1662.
- [4] D. Bernoulli and S. Blower, “An attempt at a new analysis of the mortality caused by smallpox and of the advantages of inoculation to prevent it,” Reviews in Medical Virology, vol. 14, no. 5, p. 275, 2004.
- [5] T. R. Malthus, D. Winch, and P. James, Malthus: ‘An Essay on the Principle of Population’. Cambridge University Press, 1992.
- [6] B. Gompertz, “On the nature of the function expressive of the law of human mortality, and on a new mode of determining the value of life contingencies,” Philosophical Transactions of the Royal Society of London, no. 115, pp. 513–583, 1825.
- [7] R. Zwanzig, “Generalized Verhulst laws for population growth,” Proceedings of the National Academy of Sciences, vol. 70, no. 11, pp. 3048–3051, 1973.
- [8] W. O. Kermack and A. G. McKendrick, “A contribution to the mathematical theory of epidemics,” Proceedings of the Royal Society of London. Series A, vol. 115, no. 772, pp. 700–721, 1927.
- [9] L. J. Allen, F. Brauer, P. Van den Driessche, and J. Wu, Mathematical Epidemiology, vol. 1945. Springer, 2008.
- [10] F. Brauer, “Compartmental models in epidemiology,” in Mathematical Epidemiology, pp. 19–79, Springer, 2008.
- [11] F. Brauer, “The Kermack–McKendrick epidemic model revisited,” Mathematical Biosciences, vol. 198, no. 2, pp. 119–131, 2005.
- [12] E. Forgoston and R. O. Moore, “A primer on noise-induced transitions in applied dynamical systems,” SIAM Review, vol. 60, no. 4, pp. 969–1009, 2018.
- [13] Š. Schwabik, Generalized Ordinary Differential Equations. World Scientific, 1992.
- [14] G. T. Nieddu, “Outbreak and extinction dynamics in stochastic populations,” 2018.
- [15] E. Forgoston, S. Bianco, L. B. Shaw, and I. B. Schwartz, “Maximal sensitive dependence and the optimal path to epidemic extinction,” Bulletin of Mathematical Biology, vol. 73, no. 3, pp. 495–514, 2011.

- [16] I. B. Schwartz, E. Forgoston, S. Bianco, and L. B. Shaw, “Converging towards the optimal path to extinction,” Journal of The Royal Society Interface, vol. 8, no. 65, pp. 1699–1707, 2011.
- [17] G. Nieddu, L. Billings, and E. Forgoston, “Analysis and control of pre-extinction dynamics in stochastic populations,” Bulletin of Mathematical Biology, vol. 76, no. 12, pp. 3122–3137, 2014.
- [18] M. Bauver, E. Forgoston, and L. Billings, “Computing the optimal path in stochastic dynamical systems,” Chaos: An Interdisciplinary Journal of Nonlinear Science, vol. 26, no. 8, p. 083101, 2016.
- [19] G. T. Nieddu, L. Billings, J. H. Kaufman, E. Forgoston, and S. Bianco, “Extinction pathways and outbreak vulnerability in a stochastic Ebola model,” Journal of The Royal Society Interface, vol. 14, no. 127, p. 20160847, 2017.
- [20] L. Billings and E. Forgoston, “Seasonal forcing in stochastic epidemiology models,” Ricerche di Matematica, vol. 67, no. 1, pp. 27–47, 2018.
- [21] D. T. Gillespie, “Exact stochastic simulation of coupled chemical reactions,” The Journal of Physical Chemistry, vol. 81, no. 25, pp. 2340–2361, 1977.
- [22] C. W. Gardiner et al., Handbook of Stochastic Methods, vol. 3. springer Berlin, 1985.